Kinetics of intercalation of tetraalkylammonium ions into polyacetylene

Francis Ignatious, Bernard François and Claude Mathis*
Institut Charles Sadron (CRM-EAHP) (CNRS-ULP), 6 rue Boussingault, 67083 Strasbourg, France
(Received 22 March 1989; revised 6 September 1989; accepted 12 September 1989)

The doping kinetics of Shirakawa polyacetylene (PA), involving bulky R_4N^+ like Bu_4N^+, Hep_4N^+ and $Dodec_4N^+$, was undertaken. From the drastic influence of dopant concentration and film thickness on the kinetics, the interfibrillar diffusion of the dopant was identified as the rate-limiting step. However, a minimum value of 10^{-15} cm^2 s^{-1} was estimated for the intrafibrillar diffusion constant. The relaxation of the narrow electron spin resonance line, produced during a short heterogeneous doping of *cis*-PA, was critically examined in the case of each of the above cations. The relaxation times were found to decrease in the order $Bu_4N^+ < Hep_4N^+ < Dodec_4N^+$.

(Keywords: kinetics; doping; diffusion; polyacetylene)

INTRODUCTION

Conjugated organic polymers are endowed with metallic properties only when they are subjected to an oxidation or reduction process, which has been phenomenologically called doping[1]. The interesting inherent properties of the resultant product are governed essentially by the kinetics of the doping step. Most of the discrepancies pertaining to the properties of the doped product have been attributed to the inhomogeneous dopant distribution in them. This has to some extent prevented the proper advancement of the theoretical treatment of the newly emerging branch of solid-state chemistry.

The intense research activity devoted to the field of conducting polymers is due to their promising potential applications, such as solid-state batteries[2], electrochromic displays[3], microelectronics devices[4], etc. The basic concepts underlying such technological projections necessitate perfect knowledge and control of mass transport in these systems. Despite this fact, little has been done to unravel the complexities involved in the doping kinetics whereas much theoretical and experimental work deals with electronic charge transport in the resultant doped state. Even among the few studies reported, there is no agreement on the magnitude of the diffusion coefficient of ionic species in polyacetylene (PA). The estimated values[5-7] range from 10^{-9} to 10^{-18} cm^2 s^{-1}.

Such discord exists only in the case of PA synthesized by the Shirakawa technique but not in the one obtained through the Durham precursor route[8]. The major difficulty in interpreting the results in the former stems from its fibrillar morphology, which is further complicated with films having two distinct faces: upper mat and lower dense shiny surface. Moreover, extremely rigorous conditions are required for handling the highly air-sensitive PA. In spite of these difficulties, several techniques have been suitably modified so as to be appropriate to such measurements. The common methods utilized are weight uptake[9], radioisotopic tracer analysis[10], open-circuit voltage decay measurements in electrochemical cells[11] and electron microprobe analysis[12].

Recently François *et al.*[13] have developed a novel technique that involves the direct monitoring of the consumption of the carbanions, which are responsible for the reduction of PA, by observing the variation of optical density or electrical conductance of the dopant solution. This study has revealed the following facts: the rate of doping is proportional to the concentration of the dopant and inversely proportional to the square of the film thickness.

The above results unequivocally demonstrate that the overall doping kinetics are limited by the rate of penetration of the dopants in the interfibrillar space, because of the simultaneous consumption of the dopants. It is worth while noting that, due to the complex morphology of the films obtained by the Shirakawa technique, several steps participate in the doping process, viz. the interfibrillar diffusion of dopants, the kinetics of electron transfer at the surface of fibrils, the migration of the doped site along with its counter-cation into the fibrils and finally simultaneous or further reorganization and crystallization of the doped fibrils.

Most of the confusion displayed in the experimentally assessed diffusion coefficients originates from the difficulty in ascertaining which of the above-enumerated steps is the rate-controlling one. The above investigation, in the case of alkali metals, has undoubtedly shown that the doping kinetics are governed by the rate of interfibrillar diffusion, thereby making the rate of ion transport in the doped state inaccessible to direct experimental measurement. These observations encouraged us to undertake the study of the doping kinetics of insertion of bulky tetraalkylammonium ions (R_4N^+), which might drastically diminish intrafibrillar diffusion, so as to render it preponderant and hence available to experimental determination. The insertion of R_4N^+ ions envisages the utilization of a complex carbanionic dopant system[14].

This work is presented in two sections: the first deals

* To whom correspondence should be addressed.

0032-3861/90/061108-08

with investigation of the overall doping kinetics as a function of the size of R_4N^+ ions by making use of the optical spectroscopic technique[13] and the second describes an electron spin resonance technique, put forward by Rachdi *et al.*[15], which looks into the solid-state diffusion of R_4N^+ ions in PA.

EXPERIMENTAL

Synthesis of PA films

Synthesis of PA films was carried out at −78°C, using a modified Shirakawa technique[17]. The concentration of the catalyst mixture in pentane and the rate of acetylene flow were adjusted to avoid the formation of the dense, shiny surface. Large homogeneous samples of varying thicknesses but of constant density (around 0.2 g cm^{-3}) were prepared. The washed and dried films were kept in sealed tubes at −30°C. The films were handled in a high-quality dry box (<0.2 ppm O_2 and <1 ppm H_2O).

Synthesis of dopant system

The dopant system consists of a mixture of barium benzophenone (BaBz) dianion in tetrahydrofuran (THF) and R_4NBr. The BaBz dianion was synthesized as described earlier[14]. The tetraalkylammonium salts were purchased from Fluka. They were dried under vacuum (<10^{-4} mmHg) at 80°C for at least 12 h and were kept in sealed tubes provided with breakseals.

Determination of interfibrillar diffusion constant (D_1)

This was performed in an apparatus consisting of two compartments, 'a' and 'b', of which 'b' is provided with a conductivity cell. Discs of PA film were inserted in the opening between the two compartments. The apparatus was filled with pure THF under vacuum and a concentrated solution of R_4NBr in THF was injected into compartment 'a' at zero time. The solutions are kept under constant agitation. The quantity of R_4NBr diffusing through the PA membrane was monitored by recording the increase of conductance as a function of time. The experiment was repeated for films of different thicknesses and also for different R_4NBr.

Kinetics of doping

The kinetic measurements were performed in a specially designed and constructed glass apparatus, which was sealed under high vacuum. The main branch of the glass apparatus consists of a large cell provided with quartz optical windows of path length 2 mm. The latter, filled with dopant solution, was introduced into the thermostated cavity of a Varian 2300 u.v./vis. spectrometer. The breakseal of the tube containing the PA film was opened and the latter was moved along with a magnet and put into the dopant solution at zero time. The consumption of the dopant carbanion was recorded by noting the optical density at an appropriate wavelength as a function of time. During the entire measurement the dopant solution was kept under constant agitation. The exact concentrations of the dopant solution before and after the reaction were determined by utilizing another optical cell of path length 0.01 mm, incorporated in the same apparatus. The weights of the PA films were selected in such a way as to limit the dopant consumption to less than 10% of its original concentration. The measurements were undertaken for different dopant concentrations, different film thickness and different dopant cations.

Solid-state diffusion of R_4N^+ ions

The e.s.r. spectra were recorded using a Bruker ESP 300 spectrometer. The glass apparatus used for the study is shown in *Figure 1*. In the dry box, the glass apparatus was filled with a small piece of *cis*-PA film and subsequently transferred to a vacuum line and sealed. Since the experiment involves a comparison of the diffusion of three R_4N^+ cations (viz. Bu_4N^+, Hep_4N^+ and $Dodec_4N^+$) in PA samples, doped partially to the same extent, precise control of the doping time is necessary. This was achieved by the following technique. The sealed glass apparatus was maintained in a vertical position and the breakseal separating the dopant solution was crushed and THF was distilled into the e.s.r. tube, by cooling the latter. Thus the film was completely soaked in THF. Subsequently the film was slowly brought to the upper part (marked A in *Figure 1*) of the e.s.r. tube by tilting the tube horizontally, taking care to avoid pouring the THF back into the glass bulb containing the dopant solution. Now the latter was brought into contact with the film for exactly 2 min and removed immediately. The film was simultaneously rinsed thoroughly with the THF conserved in the e.s.r. tube. The film was soaked in the pure THF distilled into the e.s.r. tube. The e.s.r. tube was inserted into the magnetic cavity of the e.s.r. spectrometer and the relaxation of the narrow intense line that is superimposed on the broad one of *cis*-PA was monitored as a function of time. This phenomenon was studied for all three R_4N^+ mentioned earlier. In all cases the same concentration of BaBz in THF mixed with R_4NBr in slight excess of the molar ratio was used. The PA samples were cut from the same film.

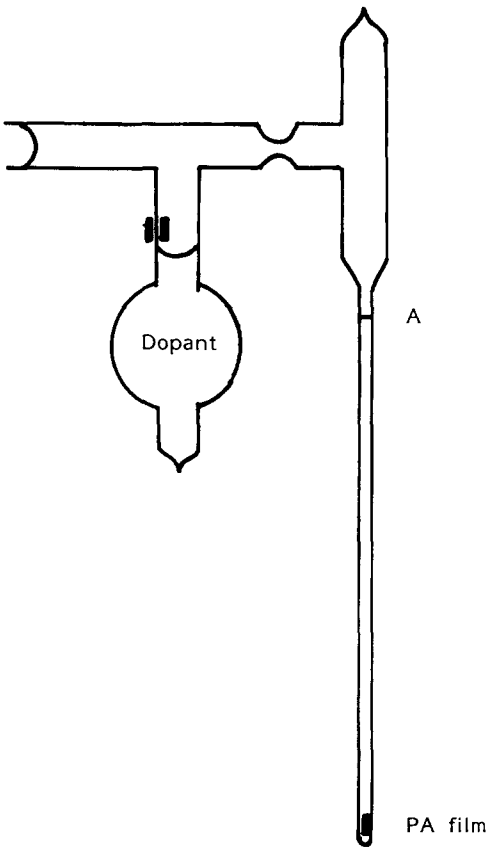

Figure 1 Glass apparatus for e.s.r. measurements

RESULTS

Interfibrillar diffusion of R_4NBr (D_I)

In order to check whether the size of the R_4NBr hinders penetration into the PA films, we have studied the diffusion of these molecules, which are not able to dope the PA. We have measured the increase of electrical conductances of THF in one compartment, due to the migration of R_4NBr from the other, through a PA membrane partition. The measured D_I values are reported in *Table 1*. The measured mean value is $D_I = 5 \times 10^{-6}\,cm^2\,s^{-1}$, which does not significantly depend on the size of the R_4NBr or the film thickness. This value is similar to those already reported for the diffusion of dodecane across a PA film determined by a gas chromatographic analysis[13].

Doping kinetics

Principle of the method. The insertion of R_4N^+ into PA requires the utilization of a carbanionic complex system, viz. barium benzophenone (BaBz) dianion mixed with an appropriate R_4NBr (BaBz/THF/R_4NBr), for the reasons already explained in ref. 14. The mechanism, elucidated by us, involves electron transfer from the benzophenone dianion to the PA, with simultaneous incorporation of R_4N^+ ions, to counterbalance the charge on the reduced PA formed. Interestingly this process is accompanied by visible spectral changes, which facilitate the easy monitoring of the doping kinetics. The dopant complex has an absorption maximum at 480 nm and it exhibits an intensity decrease during the process, while the radical anion ($\lambda_{max} = 642$ nm) formed during the reaction increases in intensity. All our kinetics measurements were performed by recording the increase of the intensity of the peak at 642 nm.

From the experimental data, the normalized doping level $Y_n = Y/Y_{max}$ (doping level at time t/maximum doping level) can be deduced and plotted as a function of time. Further, Y_n is expressed in terms of a simple diffusion process:

$$\ln[1/(1-Y_n)] = f(t)$$

Typical curves are shown in *Figure 2*. The curve is linear up to 50–80% of the maximum doping, after which there is a levelling off. The slope of this straight line is called the 'doping rate' in further discussions.

Critical concentration of R_4NBr in the dopant system. Owing to the peculiar mechanism operating during the insertion of R_4N^+ ions while utilizing BaBz/THF/R_4NBr as the dopant, the concentrations of both BaBz and R_4NBr control the rate of doping. We have studied the influence of the concentration of Hep_4NBr on the doping rate, for a constant concentration of BaBz and for pieces of PA cut from the same film. The variation of the doping rate as a function of the concentration of Hep_4NBr is depicted in *Figure 3*. It is clear that the doping rate is strongly dependent on R_4NBr concentration up to a certain point, beyond which it is almost independent. This inflection point corresponds to 2 moles of Hep_4NBr with respect to BaBz. In all further investigations R_4NBr was used in excess of the above 2:1 ratio. The molar extinction coefficient of this complex solution was estimated to be $23\,000\,l\,mol^{-1}\,cm^{-1}$ at 480 nm.

Doping kinetics as a function of cation size. The kinetics were studied for three different cations, namely Bu_4N^+, Hep_4N^+ and $Dodec_4N^+$. In all cases the influence of various parameters, like dopant concentration, thickness of the film and temperature, on the doping kinetics was examined. The results are summarized in *Tables 2* to *5*. It should be remarked that, in the case of $Dodec_4NBr$, lower concentrations of BaBz were used, due to the moderate solubility of the former in THF. Similarly the determination of the temperature dependence of the doping rate was limited to a small temperature range because of the experimental constraints imposed by the moderate stability of the dopant system above room temperature and the partial insolubility of the required quantity of R_4NBr at temperatures below −20°C.

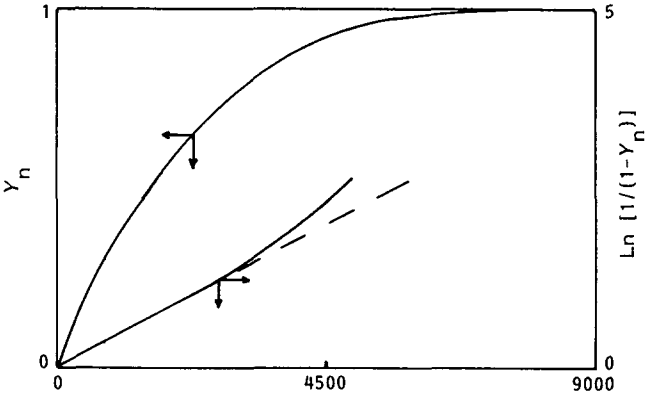

Figure 2 A typical doping curve

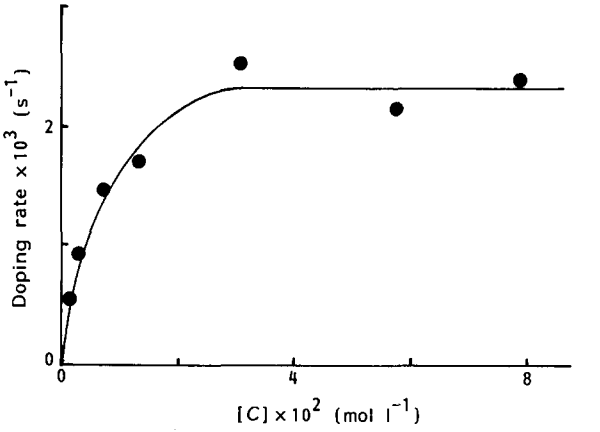

Figure 3 Variation of doping rate as a function of the concentration of Hep_4NBr, for a constant concentration of BaBz. Film thickness 110 μm, film density 0.15 g cm^{-3}

Table 1 Conductometric determination of interfibrillair diffusion constant for R_4NBr across a PA film

Salt	Film thickness (μm)	Film density (g cm^{-3})	D_I (10^{-6} cm^2 s^{-1})
Bu_4NBr	100	0.15	3.0
Bu_4NBr	160	0.16	7.5
Bu_4NBr	220	0.19	6.5
Bu_4NBr	340	0.21	8.0
Bu_4NBr	580	0.3	4.6
Hep_4NBr	340	0.21	4.3
$Dodec_4NBr$	220	0.19	3.0

Table 2 Doping kinetics of *cis*-PA films (dopant BaBz/THF/Bu_4NBr)

Dopant conc. (10^{-2} mol l^{-1})	Film thickness (μm)	Film density (g cm^{-3})	Doping rate (10^{-3} s^{-1})
1.3	160	0.16	2.8
0.7	160	0.16	1.4
0.52	160	0.16	1.2
0.22	160	0.16	0.4
1.03	220	0.19	0.87
0.84	220	0.19	0.77
0.185	220	0.19	0.14
1.35	580	0.24	0.12
0.87	580	0.24	0.095
0.60	580	0.24	0.07
0.10	580	0.24	0.017

Table 3 Doping kinetics of *cis*-PA films (dopant BaBz/THF/Hep_4NBr)

Dopant conc. (10^{-2} mol l^{-1})	Film thickness (μm)	Film density (g cm^{-3})	Doping rate (10^{-3} s^{-1})
0.47	110	0.15	1.85
0.42	110	0.15	1.69
0.29	110	0.15	1.10
1.15	220[a]	0.19	0.98
0.78	220	0.19	0.72
0.57	220	0.19	0.54
0.36	220	0.19	0.32
0.95	340	0.21	0.195
0.80	340	0.21	0.14
0.22	340	0.21	0.05
1.45	550	0.24	0.09
1.10	550	0.24	0.024
0.54	550	0.24	0.035
0.39	550	0.24	0.025

[a] *Trans* isomer

Table 4 Doping kinetics of *cis*-PA films (dopant BaBz/THF/$Dodec_4NBr$)

Dopant conc. (10^{-2} mol l^{-1})	Film thickness (μm)	Film density (g cm^{-3})	Doping rate (10^{-3} s^{-1})
0.418	110	0.15	1.32
0.245	110	0.15	0.75
0.166	110	0.15	0.34
0.49	220	0.19	0.66
0.308	220	0.19	0.39
0.193	220	0.19	0.22

Table 5 Doping kinetics of *cis*-PA films as a function of temperature (dopant BaBz/THF/Hep_4NBr; film thickness 220 μm; film density 0.19 g cm^{-3})

Dopant conc. (10^{-2} mol l^{-1})	Temperature (μm)	Doping rate (10^{-3} s^{-1})	Doping rate corrected[a] (10^{-3} s^{-1})
7.82	19.4	1.12	1.12
6.24	10.7	0.58	0.72
5.61	0.30	0.33	0.45
4.82	−17.4	0.096	0.15

[a] Taking into account the decrease of dopant concentration

Figures 4 to *6* illustrate the variation of the doping rate as a function of the concentration of the dopant. It can be seen from the figures that the doping rates are proportional to the dopant concentration. Films having the same thickness fall on a straight line. The slopes of the latter are inversely proportional to the thickness of the film, as shown in *Figure 7*. For comparison, experimental results regarding lithium and potassium doping taken from ref. 16 are also indicated in the figure. The fact that all the experimental results fall on the same curve shows that the doping rate is independent of the cation size.

Figure 8 shows the Arrhenius plot for the variation of doping rate as a function of temperature. From its slope an activation energy of about 5.9 kcal mol^{-1} is obtained.

The experimental data presented above lead to the following conclusions:

(a) The doping rate is proportional to the concentration of the dopant solution.

(b) For a fixed dopant concentration, the doping rate is inversely proportional to the square of the film thickness.

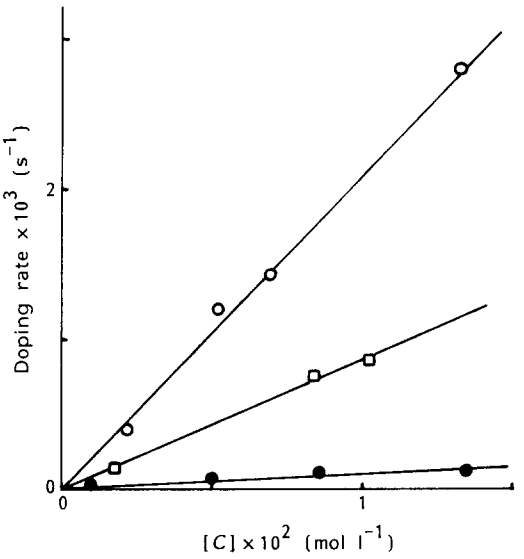

Figure 4 Linear relationship between the doping rate and the dopant concentration. Dopant BaBz/THF/Bu_4NBr. *Cis*-PA films of thickness 160 μm (○) 220 μm (□) and 580 μm (●)

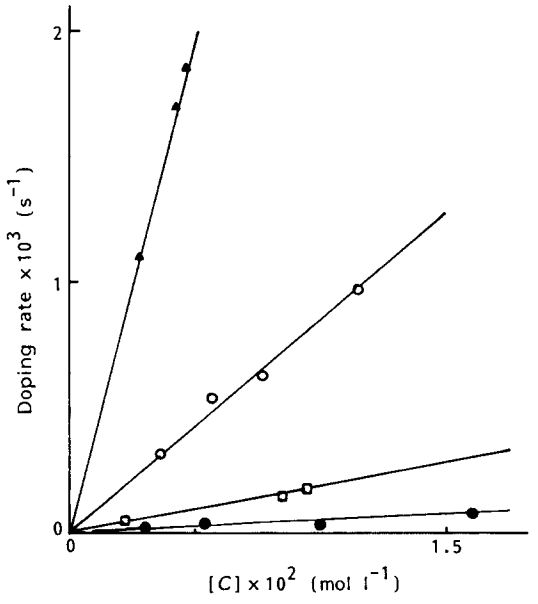

Figure 5 Linear relationship between the doping rate and the dopant concentration. Dopant BaBz/THF/Hep_4NBr. *Cis*-PA films of thickness 110 μm (▲), 220 μm (○), 380 μm (□) and 550 μm (●)

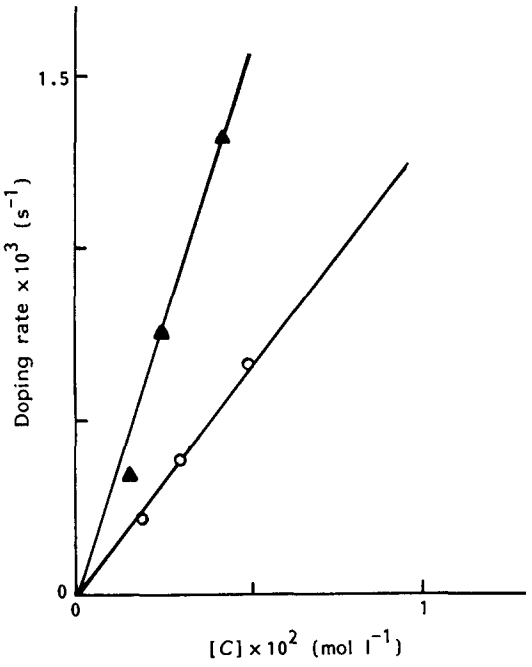

Figure 6 Linear relationship between the doping rate and the dopant concentration. Dopant BaBz/THF/Dodec$_4$NBr. *Cis*-PA films of thickness 110 μm (▲) and 220 μm (○)

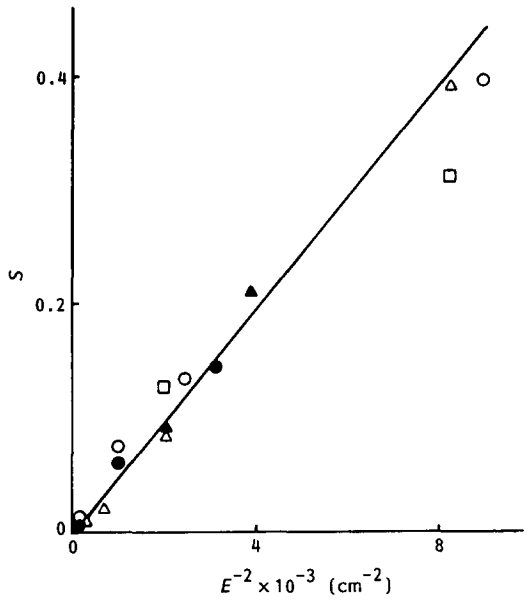

Figure 7 Linear relationship between the slope of the plot of doping rate as a function of the dopant concentration and the inverse of the squared film thickness: (●) Li^+, (○) K^+, (▲) Bu_4N^+, (△) Hep_4N^+ and (□) $Dodec_4N^+$

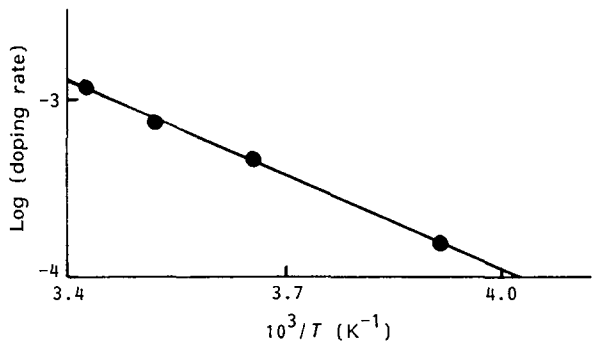

Figure 8 Variation of doping rate as a function of temperature: dopant BaBz/THF/Hep$_4$NBr, film thickness 220 μm

(c) The doping rate is independent of the size of the dopant counterions like Li^+, K^+, Bu_4N^+, Hep_4N^+ or $Dodec_4N^+$.

(d) The doping kinetics are similar for the *cis* and *trans* isomers.

(e) The overall doping phenomenon is governed by a weak activation energy.

These conclusions show that, even in the case of bulky counterions like $Dodec_4N^+$, the intrafibrillar diffusion constant (D_F) does not become low enough to make it the rate-determining one among the different steps participating in the doping kinetics. Therefore, even in this case, the intrafibrillar diffusion constant cannot be determined directly by this experimental technique.

Despite this difficulty, a minimum value for the intrafibrillar diffusion constant can be roughly estimated from the experimental observations by making the assumption that, in the fastest doping reaction, the observed kinetics is entirely controlled by intrafibrillar diffusion. In this work the shortest doping time was about 1000 s, leading to $D_F = 10^{-15}\,cm^2\,s^{-1}$ for a fibril diameter (d) of 200 Å using the crude approximation $(d/2)^2 = Dt$. But it should be noted that the doping time (time to reach about 95% of doping) is directly proportional to the dopant concentration. In the case of the complex dopant system, BaBz/THF/R_4NBr, concentrations higher than $10^{-2}\,mol\,l^{-1}$ cannot be used due to the partial insolubility of R_4NBr. In the case of alkali-metal doping, where dopant concentrations about one order of magnitude higher can be used, doping times of about 1 min could be measured, giving an estimation of $10^{-14}\,cm^2\,s^{-1}$ for the lower limit of D_F (ref. 16). So the actual value of the intrafibrillar diffusion coefficient is much higher than most values reported in the literature for Shirakawa PA and is comparable to that already reported in the case of Durham PA[8,18]. In the PA prepared by this technique, owing to its non-fibrillar morphology, there is no confusion as to the appropriate dimension, which should be taken into account to assess the diffusion constant.

Even though an approximate determination of the controversial intrafibrillar diffusion constant is possible by the u.v./vis. spectroscopic technique, it might be interesting to make a direct determination of this parameter. Therefore we have resorted to the e.s.r. technique described in the literature[15] to evaluate this diffusion constant, which turns out to be the most fundamental of all of the proposed applications of this conducting polymer.

Solid-state diffusion of R_4N^+ ions

Principle of the method. It is based on the observation that *cis*-PA, which has a broad e.s.r. linewidth ($\Delta H = 7$ G), when subjected to a short doping pulse, furnishes a narrow line superimposed on the broad one. In the absence of further doping, this narrow line relaxes completely to disappear into the broad one. Valuable information can be deduced from this phenomenon, based on a suitable model.

Experimental results. *Figure 9a* shows a typical e.s.r. spectrum of pristine *cis*-PA. After 2 min of contact with the dopant BaBz/THF/Bu_4NBr, a narrow line is produced, superimposed on the initial broad one (*Figure 9b*). A similar line is observed when the experiment was repeated with other counterions like Hep_4N^+ or

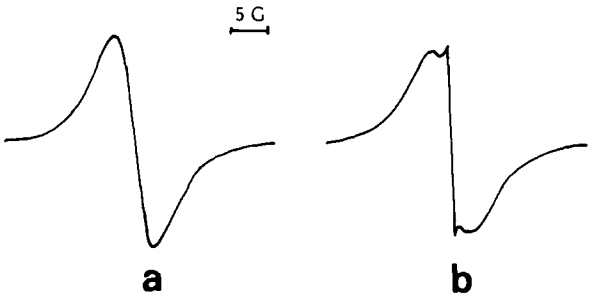

Figure 9 E.S.R. spectra of (a) *cis*-PA and (b) *cis*-PA subjected to doping for 2 min (dopant BaBz/THF/Bu_4NBr)

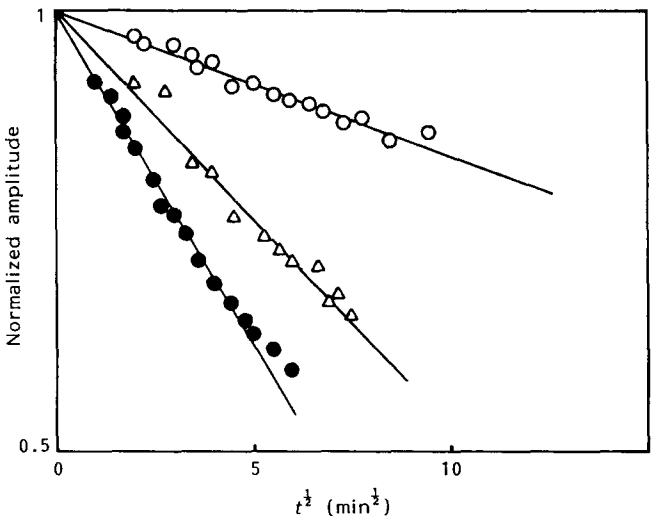

Figure 10 Variation of normalized amplitude of narrow line during its relaxation as a function of square root of time: (●) Bu_4N^+, (△) Hep_4N^+ and (○) $Dodec_4N^+$

$Dodec_4N^+$. In this comparative study, extreme care was taken to achieve the same initial doping for all three R_4N^+ ions used. For that, the doping time (2 min), the dopant concentration and the film characteristics are kept unchanged. The amplitude of the narrow line was monitored as a function of time. *Figure 10* illustrates the variation of normalized amplitude as a function of square root of time. The linear relationship is characteristic of a simple diffusion process. From *Figure 10* it is evident that the diffusion rates diminish as a function of counterion size, $Dodec_4N^+ < Hep_4N^+ < Bu_4N^+$.

Existing model. Although this double-line feature obtained during a short heterogeneous doping has been reported by several authors, in the case of both p-type[19] and n-type[20] doping of PA, it was Rachdi *et al.*[15] who quantitatively evaluated the relaxation phenomenon, to bring out a diffusion coefficient for Li^+ in PA.

The authors attributed the narrow line to undoped *trans*-PA formed during the short heterogeneous doping of *cis*-PA. Each fibril reached by the dopant is doped on its surface while *cis*-PA in it is isomerized to *trans*-PA. The relaxation of the narrow line is then attributed to electron transfer from the charged solitons on the surface of the fibrils to the neutral solitons in the core, leading to the disappearance of the undoped *trans*-PA. Using this model, they calculated a solid-state diffusion coefficient for solvated Li^+ ($D_F = 2 \times 10^{-17}$ cm^2 s^{-1}). Resting solely on this model, D_F values of the same order of magnitude can be deduced from our results.

The above model provides easy access to the diffusion constants for counterions in PA fibrils, but the D_F values obtained are in disagreement with the results of the kinetic study presented in the section on 'Doping kinetics' above. Therefore we have checked the validity of the model, to find out to what extent it is capable of satisfying all the experimental observations.

Davidov *et al.*[19] observed this narrow-line spectrum superimposed on the broad line for both *cis* and *trans* isomers. Furthermore they have characterized this narrow line by studying its thermal behaviour. From the thermal dependence of its linewidth and intensity, they have assigned the narrow line to a doped metallic phase. Similarly Foot *et al.*[21] have reported similar two-line spectra for *trans*-PA samples prepared by the Durham route when subjected to a short AsF_5 or lithium doping. They have further reported a D_F value of 10^{-13} cm^2 s^{-1}, from the relaxation study.

Similarly we have carried out a short heterogeneous doping on Durham *trans*-PA, which has an initial linewidth of $\Delta H = 8$ G. The dopant is benzophenone dianion in THF. This gives rise to the double-line spectrum presented in *Figure 11*. Hence it may be concluded that the narrow line arises from the doped *trans*-PA formed during heterogeneous doping. The linewidth of the narrow line observed in the case of R_4N^+ or Li^+ ions, which are the same as in their completely doped state (in the presence of THF), supports the above conclusion.

Moreover, in the case of higher alkali-metal (K,Cs,Rb) doped PA, prepared by the vapour-phase technique, where the heavily doped PA has a much larger linewidth due to the spin–orbit coupling contribution, Billaud *et al.*[22] observed a broad intense line superimposed on the narrow one of the initial *trans*-PA. From a detailed study of the thermal behaviour of these lines, they attributed the broad line to the conduction electrons and hence to the doped *trans*-PA formed in the highly doped parts of the sample.

DISCUSSION

The minimum value of D_F estimated from the experimental results from the u.v./vis. spectroscopic technique may be compared with the values reported in the literature[5–7]. As already cited, the values differ by nine orders of magnitude. The highest value (10^{-8} cm^2 s^{-1}) is a macroscopic diffusion coefficient, determined by making the simplified assumption that the fibrillar PA sample is a bulk sheet. Will[23] reported a D_F value of

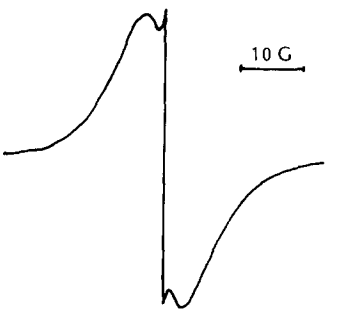

Figure 11 E.S.R. spectrum of Durham *trans*-PA subjected to short doping for 2 min (dopant Na_2Bz/THF)

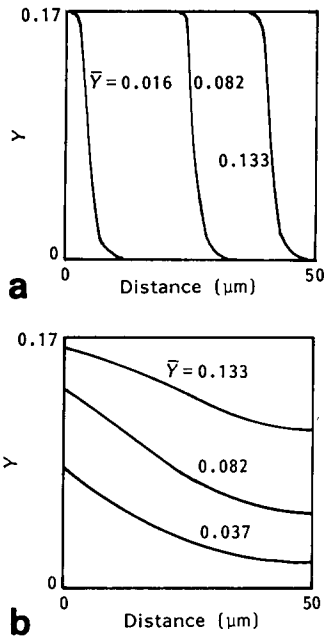

Figure 12 Computed distributions of doped sites across half films at three doping levels with (a) $D_F = 10^{-12}\,cm^2\,s^{-1}$ and (b) $D_F = 10^{-14}\,cm^2\,s^{-1}$ for film thickness 100 μm

$5.7 \times 10^{-12}\,cm^2\,s^{-1}$ for the diffusion of BF_4^-. He explained the low D_F values ($< 10^{-17}\,cm^2\,s^{-1}$) as due to the poor wetting of the fibrils. In our case there is no such wetting problem but the experimental technique does not permit direct determination of the exact value. In fact, the real value is even higher than $10^{-15}\,cm^2\,s^{-1}$. Furthermore these high values are attested by similar ones reported in the case of Durham PA, where no ambiguity exists.

This high value of D_F has a direct impact on the dopant distribution profiles, which are presented in *Figure 12*. These were obtained in the case of potassium doping, by simulation of a theoretical model. The model takes into account the apparent density of the films, the maximum doping levels and the inter- and intrafibrillar diffusion coefficients. Except for the D_F value, all others are experimentally determinable. These values along with the minimum estimated D_F values are used to compute the diffusion profiles. *Figure 12* brings out clearly the contrast between the profiles, if the D_F values were respectively (a) 10^{-12} or (b) $10^{-14}\,cm^2\,s^{-1}$. These profiles reveal the highly inhomogeneous distribution of doped sites, at intermediate doping levels. This behaviour was already observed directly by electron microprobe analysis of iodine distribution in PA[1]. Therefore it becomes impossible to achieve a homogeneous dopant distribution at intermediate doping levels by simple control of doping time and dopant concentration.

This serious handicap of heterogeneous dopant distribution at intermediate levels can be overcome by performing thermodynamic control of the dopant levels. It consists of utilizing suitable carbanionic salts having appropriate redox potentials corresponding to those of doped PA at a predetermined level, and allowing the reaction to proceed to completion. This has already been verified in the case of potassium doping[24]. A set of carbanionic salts in THF and in a non-polar medium for lithium doping have been tested and will be reported elsewhere. The lithium doping in non-polar solvent is of great interest since it avoids all extraneous effects arising from solvent co-insertion.

Such thermodynamic control of doping levels in the case of R_4N^+ doping seems to be difficult to realize for several reasons. When doped above 8%, the R_4N^+ doped PA becomes unstable[25]. Below 8%, even though several dopant systems were used[14], the variety of their redox potentials is not sufficient to furnish the desired doping level. If proper purification of the R_4NBr can be effected, the ion-exchange technique presented in ref. 25 turns out to be the best method to achieve intermediate doping levels.

In the light of the diffusion profiles discussed in the above section, the e.s.r. spectral characteristics of heterogeneously doped PA can be understood. During the short doping pulse, the dopant molecules penetrate into the film and encounter the fibril, on whose surface electron transfer occurs. Owing to the D_F value of around $10^{-13}\,cm^2\,s^{-1}$, it takes only a few seconds for the doped sites to reach the centre of the fibril, which is doped to the maximum doping level permitted by the redox potential of the dopant. So all the dopant molecules flowing into the film at a fairly high rate ($D_I = 10^{-6}\,cm^2\,s^{-1}$) react within a very short distance from the surface of the film, leaving behind a fully doped phase, and the pure solvent, devoid of the reactive carbanions, continues to advance into the film. For a short doping pulse, only a very limited portion of the fibrillar structure is touched. This gives rise to the observed double-line spectrum.

The relaxation of the narrow-line e.s.r. spectrum can be interpreted as follows. The doped phase formed during the short doping is in contact with non-doped *cis*-PA, such that electron transfer followed by counterion diffusion occurs from the doped to the pure PA, leading to the relaxation of the narrow line into the broad one. Therefore, diffusion occurs along the fibril direction and not across the fibril diameter. The main drawback of this picture is that it does not furnish any clue to the diffusion coefficient, due to lack of knowledge of the diffusion length.

CONCLUSIONS

The outcome of this investigation is that, even in the case of bulky cations like $Dodec_4N^+$, the intrafibrillar diffusion coefficient does not reach the reported low values such as $10^{-18}\,cm^2\,s^{-1}$. In fact the actual values are higher than $10^{-15}\,cm^2\,s^{-1}$, the minimum value estimated by our experimental technique. Such high values exclude any possibility of homogeneous doping at intermediate doping levels by simple control of doping time or dopant concentration, as is usually the case. Instead, thermodynamic control of doping is necessary if homogeneous doping at intermediate levels is desired. This high value is well suited to the predicted applications of PA as electrodes in rechargeable batteries but is unsuited for n–p junctions.

REFERENCES

1 Pekker, S. and Janossy, A. 'Handbook of Conducting Polymers' (Ed. T. A. Skotheim), Marcel Dekker, New York, 1986, Vol. 1
2 MacDiarmid, A. G. and Maxfield, M. 'Electrochemical Science and Technology of Polymers–1', Elsevier Applied Science, London, 1987, p. 67

3 Kobayashi, T., Yoneyama, H. and Tamura, H. *J. Electroanal. Chem.* 1984, **177**, 281
4 Paul, E. W., Ricco, A. J. and Wrighton, M. A. *J. Phys. Chem.* 1985, **89**, 1441
5 Schlenoff, J. B. and Chien, J. C. W. *J. Am. Chem. Soc.* 1987, **109**, 6269
6 Berniere, F., Haridoss, S., Louboutin, J. P., Aldissi, M. and Fabre, J. M. *J. Phys. Chem. Solids* 1981, **42**, 649
7 Kaneto, K., Maxfield, M., Nairns, D. P. and MacDiarmid, A. G. *J. Chem. Soc., Faraday Trans. (I)* 1982, **78**, 3417
8 Foot, P. J., Mohammed, F., Calvert, P. D. and Billingham, N. C. *J. Phys. (D) Appl. Phys.* 1987, **20**, 1354
9 Danno, T., Miyasaka, K. and Ishikawa, K. *J. Polym. Sci., Polym. Phys. Edn.* 1983, 21, 1521
10 Berniere, F. and Pekker, S. *Solid State Commun.* 1986, **57**, 835
11 Kaner, R. B. and MacDiarmid, A. G. *J. Chem. Soc., Faraday Trans. (I)* 1984, **80**, 2109
12 Janossy, A., Pogany, L., Pekker, S. and Swietlik, R. *Mol. Cryst., Liq. Cryst.* 1981, **77**, 185
13 François, B., Mathis, C. and Nuffer, R. *Synth. Met.* 1987, **20**, 311
14 Ignatious, F., François, B. and Mathis, C. *Makromol. Chem.* 1989, **190**, 737
15 Rachdi, F., Bernier, P., Faulques, E., Lefrant, S. and Schué, F. *J. Chem. Phys.* 1984, **80**, 62
16 Mathis, C., Nuffer, R., Rudatsikira, A. and François, B. *Makromol. Chem., Macromol. Symp.* 1989, **24**, 99
17 Ito, T., Shirakawa, H. and Ikeda, S. *J. Polym. Sci., Polym. Chem. Edn.* 1974, **12**, 11
18 Mathis, C., Weizenöfer, R., Lieser, G., Enkelmann, W. and Wegner, G. *Makromol. Chem.* 1988, **189**, 2617
19 Davidov, D., Roth, S. and Weumann, W. *J. Phys. (Paris) Coll.* 1983, **44**, C3, 295
20 Francois, B., Bernard, M. and André, J.-J. *J. Chem. Phys.* 1981, **75**, 4142
21 Foot, P. J. S., Billingam, N. C. and Calvert, P. D. *Synth. Met.* 1986, **16**, 105
22 Billaud, D., Ghanbaja, J., Mareche, J. F., McRae, E. and Goulon, C. *Synth. Met.* 1988, **24**, 23; Ghanbaja, J., Goulon, C., Mareche, J. F. and Billaud, D. *Solid State Commun.* 1987, **64**, 69
23 Will, F. G. *J. Electrochem. Soc., Electrochem. Sci. Technol.* 1985, **132**, 745
24 François, B. and Mathis, C. *Synth. Met.* 1986, **16**, 105
25 Ignatious, F. and Mathis, C. *Macromolecules* 1990, **23**, 70